

Article

An Interface Pressure Detection Method of Cable Silicone Rubber-XLPE Based on Nonlinear Ultrasound

Chunhua Fang^{1,2,*}, Jianben Liu¹, Aoqi Sun², Junxiong Wu², Rong Xia¹, Benhong Ouyang¹, Yilin Zhang² and Fang Li²

¹ State Key Laboratory of Power Grid Environmental Protection, China Electric Power Research Institute Co., Ltd., Wuhan 430074, China

² School of Electrical Engineering and New Energy, China Three Gorges University, Yichang 443002, China

* Correspondence: fang107531@163.com

Abstract: The interface pressure between the cable attachment and the body is crucial for the stable long-term operation of the cable. To solve the issue of interface insulation characteristics' damage caused by the pressure transducer measurement method, a non-destructive testing method of silicone rubber interface pressure using nonlinear ultrasound is presented. Initially, the study analyzes the propagation characteristics of ultrasonic waves at the interface of cross-linked polyethylene and silicone rubber. The study also establishes the relationship between the nonlinear coefficient and the interface pressure. Subsequently, a nonlinear ultrasonic test platform is constructed using the pulse reflection method to measure the interface pressure of flat silicone rubber and cross-linked polyethylene through nonlinear ultrasonic testing. Theoretical and experimental results indicate that the fundamental amplitude of the frequency domain of the interface reflection wave decreases, and the second harmonic amplitude and nonlinear coefficient both increase as pressure increases. These results demonstrate that the nonlinear ultrasound, non-destructive testing method can accurately evaluate the interfacial pressure state of the cable accessories.

Keywords: cable; silicone rubber; nonlinear ultrasound; interfacial pressure; nonlinear coefficient



Citation: Fang, C.; Liu, J.; Sun, A.; Wu, J.; Xia, R.; Ouyang, B.; Zhang, Y.; Li, F. An Interface Pressure Detection Method of Cable Silicone Rubber-XLPE Based on Nonlinear Ultrasound. *Appl. Sci.* **2023**, *13*, 5404. <https://doi.org/10.3390/app13095404>

Academic Editor: Mário João S. F. Santos

Received: 9 April 2023
Revised: 20 April 2023
Accepted: 24 April 2023
Published: 26 April 2023



Copyright: © 2023 by the authors. Licensee MDPI, Basel, Switzerland. This article is an open access article distributed under the terms and conditions of the Creative Commons Attribution (CC BY) license (<https://creativecommons.org/licenses/by/4.0/>).

1. Introduction

With the continuous deepening of China's urbanization process, the scale of urban power grid cable equipment is constantly increasing. According to statistics, in addition to external damage, 70% of cable faults are caused by cable accessory faults [1]. The silicone rubber cross-linked polyethylene (XLPE) composite interface between the cable accessories and the body is a high incidence of cable line faults due to the concentration of stress in the electric field and the occurrence of partial discharge, leading to insulation breakdown [2]. Studies have shown that the interface pressure distribution between cable accessories and the body is between 0.10 MPa and 0.25 MPa to ensure the stable operation of the cable line [3].

The main methods for detecting the pressure at the interface between the cable attachment and the body are the sensor method [4–7] and the finite element analysis method [8–10]. The built-in sensor method is to pre-install a pressure sensor between the cable attachment and the body, and the sensor detects the pressure change at the interface and outputs the result. As this method not only requires a high-pressure sensor size specification, but also destroys the insulation characteristics between the cable attachment and the body, it is not applicable to the interface pressure measurement of cable attachments with voltage levels above 10 kV. The external fiber optic curvature sensor method is based on the outer curvature–radial displacement interface pressure relationship model of the cable accessory calibrated fiber optic sensor, which is tangentially applied to the outer layer of the accessory along the outer diameter to measure the curvature and thus obtain the interface pressure value. However, this method has only been studied for 10 kV cable accessories,

and the repeatability and stability of the sensor measurements are still in the laboratory optimization stage. The finite element analysis method uses simulation software to create a three-dimensional model of the cable joint to analyze the effect of overfill, temperature, and other factors on the interface pressure. Although the finite element analysis is a simple method, there are errors between the simulation parameters and the actual cable, and the simulation results need to be compared with the test results for verification. In summary, the existing methods for testing the interface pressure of cable accessories have their own limitations, so there is an urgent need to introduce a new method to test the interface pressure of cable accessories in the field of cable transportation and inspection.

In recent years, nonlinear ultrasound techniques have been increasingly applied to stress detection. Scholars have built stress detection platforms based on nonlinear ultrasound have conducted a large number of studies on interface adhesion [11], aluminum alloy surface stress [12], aluminum plate pre-stress [13], metal material internal stress [14,15], metal plate residual stress [16], and metal contact interface stress [17]. Mao et al. [18] combined the LCR wave method with nonlinear ultrasound techniques to evaluate the internal stresses in metallic materials under pre-stress loading conditions. The pre-stress within the metal was also detected along three directions, respectively. The experimental results showed that the second-order relative nonlinear coefficients monotonically increased with stress, and the normalized relationship was consistent with a simplified dislocation model, verifying the reliability of the method. Yan et al. [15,19] found that when tensile stress is applied to a metallic material, it affects the ultrasonic nonlinear properties in addition to the propagation velocity of the ultrasonic waves inside. Payan et al. [20] used ultrasonic methods to detect stresses in concrete, taking into account the third-order elastic constants, providing an effective method for concrete stress detection. Kim et al. found that the second harmonic generated by ultrasonic waves passing through a metal contact interface increases and then decreases with the interface pressure, reaching a maximum at a specific pressure value [17]. Jiao Jinping et al. used both linear ultrasound and nonlinear ultrasound based on the transmission method to detect the pressure at metal contact interfaces and showed that the ultrasonic nonlinear coefficient decreases with increasing interface pressure [21], and that the nonlinear characteristic parameter (nonlinear coefficient) is more sensitive to changes in interface pressure than the linear ultrasound characteristic parameter (first-order stiffness coefficient) over a small pressure variation range [22].

However, most of the current research on nonlinear ultrasonic detection of stresses at contact interfaces is aimed at metal–metal contact interfaces or metal–nonmetal interfaces. Nonlinear ultrasonic detection of stresses at nonmetal–nonmetal contact interfaces is less common. The authors based this study on nonlinear ultrasonic technology to detect the stress at the silicone rubber-XLPE interface. It not only expands the nonlinear ultrasonic detection of stress at the nonmetal–nonmetal contact interface, but also provides a possibility for the non-destructive detection of pressure at the interface between cable accessories and the body.

A non-destructive testing method for the interface pressure of cable accessories based on nonlinear ultrasound is proposed to address the limitations of existing measurement methods for measuring the interface pressure of cable accessories. Firstly, the propagation mechanism of ultrasonic waves at the interface of silicone rubber-XLPE is simulated and analyzed, and the relationship between the nonlinear coefficient and the interfacial pressure is obtained. Then, the curved structure of the cable accessory and the body is simplified to a flat structure, and the nonlinear ultrasonic test platform is built based on the ultrasonic pulse reflection method, with silicone rubber and XLPE as the research objects. The ultrasonic response under different pressures is then evaluated.

2. Finite Element Simulation

2.1. Theory

As the surface of objects have a certain degree of roughness, the contact interface is actually the contact of the rough peaks of the object surface. The uncontacted part of the interface is the air gap. This is shown in Figure 1. When pressure is applied, the contact interface undergoes intense collision and deformation, resulting in elastic and plastic deformations [17]. When the ultrasonic longitudinal wave propagates in one dimension at the contact interface, the reflected wave expression is as outlined in the equations below [23].

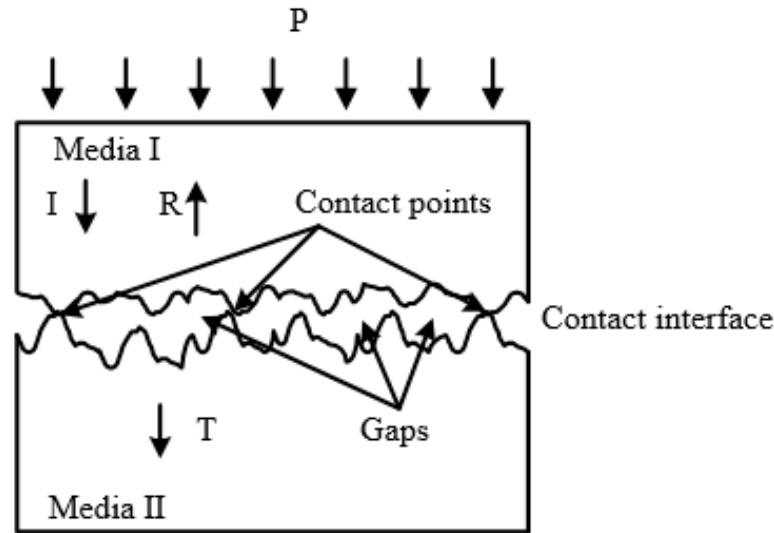


Figure 1. Ultrasonic wave propagation at the pressure-bearing interface.

$$U_R = -\frac{K_2 A_0^2}{K_1(1+4K_1^2/(\rho c\omega)^2)} - \frac{A_0 \sin(\omega t + \delta_1)}{\sqrt{1+4K_1^2/(\rho c\omega)^2}} + \frac{K_2 A_0^2 \sin(2\omega t - 2\delta_1 + \delta_2)}{\rho c\omega(1+4K_1^2/(\rho c\omega)^2)\sqrt{1+K_1^2/(\rho c\omega)^2}} \quad (1)$$

$$\delta_1 = \tan^{-1} \frac{\rho c\omega}{2K_1} \quad (2)$$

$$\delta_2 = \tan^{-1} \frac{K_1}{\rho c\omega} \quad (3)$$

$$K_1 = CP^m \quad (4)$$

$$K_2 = \frac{1}{2}mC^2P^{2m-1} \quad (5)$$

where:

A_0 is the incident wave displacement amplitude,

K_1 is the interfacial linear stiffness,

K_2 is the interfacial nonlinear stiffness,

c is the longitudinal wave speed,

ρ is the material density,

ω is the incident angular frequency,

P is the pressure,

C and m are the constants associated with the surface roughness of the interface.

The expressions for the fundamental wave amplitude and the second harmonic amplitude in the reflected wave are:

$$A_1 = \frac{A_0}{\sqrt{1 + 4K_1^2 / (\rho c \omega)^2}} = \frac{A_0}{\sqrt{1 + 4C^2 P^{2m} / (\rho c \omega)^2}} \tag{6}$$

$$\begin{aligned} A_2 &= \frac{K_2 A_0 A_1}{\rho c \omega \sqrt{1 + 4K_1^2 / (\rho c \omega)^2} \sqrt{1 + K_1^2 / (\rho c \omega)^2}} \\ &= \frac{\frac{1}{2} m C^2 P^{2m-1} A_0 A_1}{\rho c \omega \sqrt{1 + 4C^2 P^{2m} / (\rho c \omega)^2} \sqrt{1 + C^2 P^{2m} / (\rho c \omega)^2}} \end{aligned} \tag{7}$$

where:

A_1 is the fundamental amplitude in the frequency domain of the reflected wave,

A_2 is the second harmonic amplitude in the frequency domain of the reflected wave.

The relative nonlinear coefficient of ultrasonic-reflected waves is defined as the ratio of the second harmonic amplitude to the square of the fundamental wave amplitude, as follows:

$$\beta = \frac{A_2}{A_1^2} = \frac{K_2}{\rho c \omega \sqrt{1 + K_1^2 / (\rho c \omega)^2}} = \frac{\frac{1}{2} m C^2 P^{2m-1}}{\rho c \omega \sqrt{1 + C^2 P^{2m} / (\rho c \omega)^2}} \tag{8}$$

where:

β is the ultrasonic relative nonlinear coefficient.

From Equation (6) to (8), when the ultrasonic frequency, material density, and ultrasonic propagation velocity are constant, the change of pressure will cause the change of the ultrasonic fundamental wave amplitude, second harmonic amplitude, and the ultrasonic relative nonlinear coefficient. Therefore, the nonlinear coefficient can be used to reflect the magnitude of the interface pressure.

2.2. Silicone Rubber-XLPE Contact Interface Model

Considering that the roughness of the object surfaces on both sides of the interface affects the actual contact area, the surface roughness of the silicone rubber is measured based on the white-light interference test, and its surface micromorphology is shown in Figure 2. A straight line in the x-direction is selected to measure the surface wave crest of up to 4 μm , and the distance between the wave crests is 20 μm . The surface of silicone rubber is represented by a series of semicircles with an interval of 20 μm and a radius of 4 μm to characterize its interfacial micromorphology [24]. Compared to silicone rubber, the XLPE surface roughness is much smaller, so it can be regarded as a smooth plane.

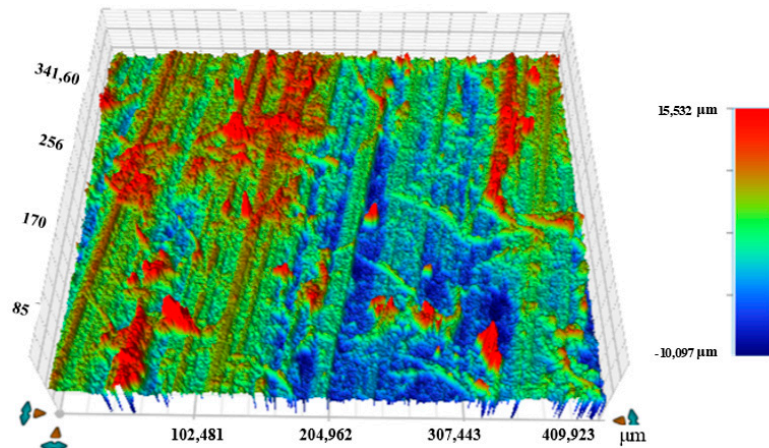


Figure 2. Silicone rubber surface micro-formation.

Figure 3 is the 2D simulation model of silicone rubber-XLPE. The top model is silicone rubber, and the bottom model is XLPE. The uncontacted part of the silicone rubber-XLPE interface is the gap, where the radius of the gap is 4 μm. In order to examine the ultrasonic nonlinear effects at the contact interface more intuitively and to reduce the computational effort, the size of the silicone rubber is 3 mm × 1 mm, and the XLPE is 3 mm × 1 mm. The modulus of elasticity of silicone rubber is 4.5 MPa, the density is 1050 kg/m³, and the Poisson’s ratio is 0.488. The modulus of elasticity of XLPE is 130 MPa, the density is 930 kg/m³, and the Poisson’s ratio is 0.32.

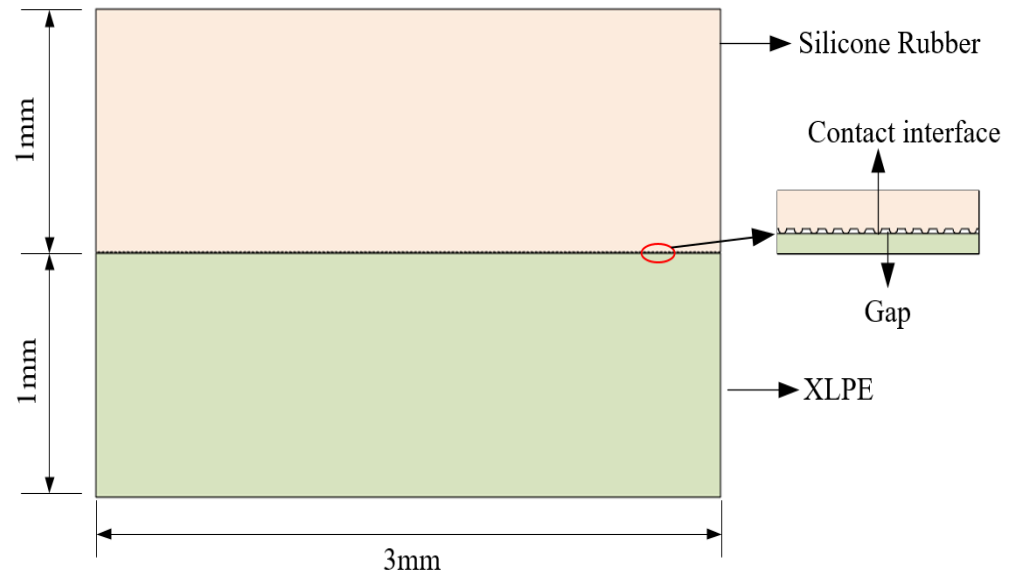


Figure 3. Silicone rubber-XLPE 2D simulation model.

The expression of the excitation source signal is shown in Equation (9). Figure 4a is the time domain waveform of the excitation source, and Figure 4b is the spectrum of the excitation source.

$$an1(t) = A_0 \sin(2\pi ft) \times e^{-((t-5T)/(T/0.5))^2} \tag{9}$$

where:

- A_0 is the amplitude of the excitation source,
- f is the center frequency of the excitation source,
- t is the time
- T is the signal period of the excitation source.

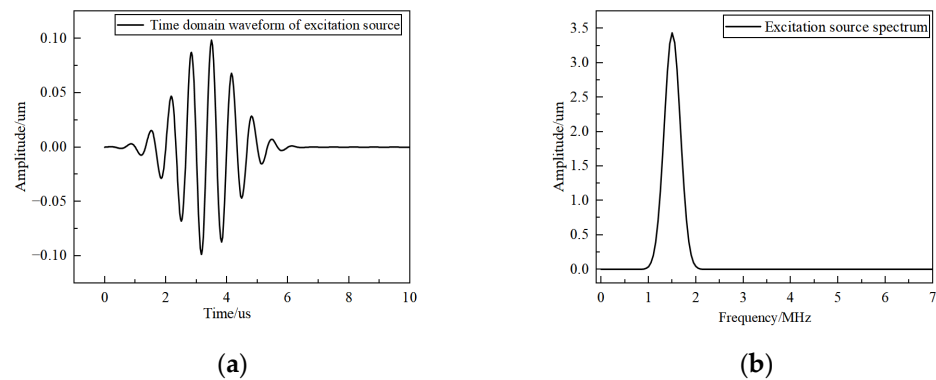


Figure 4. Excitation source spectrum. (a) Time domain waveform of the excitation source. (b) Excitation source spectrum diagram.

The finite element analysis of the silicone rubber-XLPE interface was carried out by COMSOL. The coupling of the acoustic and stress fields is carried out in two ways, direct coupling and sequential coupling. Direct coupling refers to the combined application of both pressure and ultrasonic waves into the model, facilitating transient calculations. In contrast, sequential coupling involves an initial static force analysis performed within a steady-state study. A deformation model is derived from this analysis, and it is used as the initial geometric configuration for sound field simulation calculations. The direct coupling approach in the finite element analysis of the pressure at the silicone rubber-XLPE interface was applied in this paper. A displacement load with a central frequency of 1.5 MHz was added to the upper surface of the silicone rubber to simulate the ultrasonic signal, and an upward boundary load was added to the lower surface of the XLPE to generate contact pressure on the silicone rubber-XLPE interface. Contact pairs were added to the silicone rubber-XLPE interface. Low-reflection boundaries were placed on either side of the model to reduce interference with the received signal. The maximum grid size of the simulation model is 0.02 mm, the time step is 0.05 μs , and the total simulation time is 16 μs .

2.3. Analysis of Simulation Results

Figure 5 shows the time domain diagram of the reflected waves at the silicone rubber-XLPE interface at different pressures. As the pressure increased, the reflected wave amplitude at the silicone rubber-XLPE interface slightly decreased. This is because the actual contact area of the interface increased due to pressure, the ultrasonic transmission was enhanced, and the reflection was weakened. Figure 6 shows the spectrum of the reflected waves at the silicone rubber-XLPE interface at different pressures. Comparing Figure 4b with Figure 6, the second harmonic appears in the reflected wave spectrum of the silicone rubber-XLPE interface. This indicates that a significant nonlinear effect occurred when the ultrasonic wave passed through the silicone rubber-XLPE interface. The fundamental wave amplitude and the second harmonic amplitude in Figure 6 were extracted, and the relationship between the two and the pressure at the silicone rubber-XLPE interface is shown in Figure 7a,b. The ultrasonic relative nonlinearity coefficient was calculated according to Equation (8). The relationship between it and the pressure at the silicone rubber-XLPE interface is shown in Figure 8. As the pressure increased, the fundamental amplitude of the reflected wave at the interface decreased, the second harmonic amplitude increased, and the ultrasonic nonlinearity coefficient increased. The nonlinear coefficient steeply increased at first, and then more slowly.

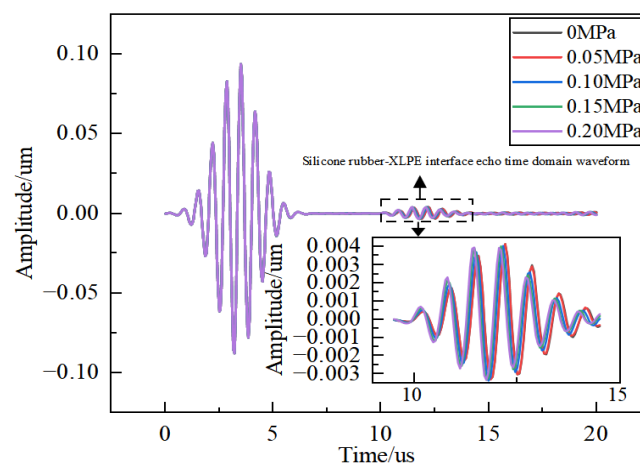


Figure 5. Silicone rubber-XLPE interface echo time domain waveform at different pressures.

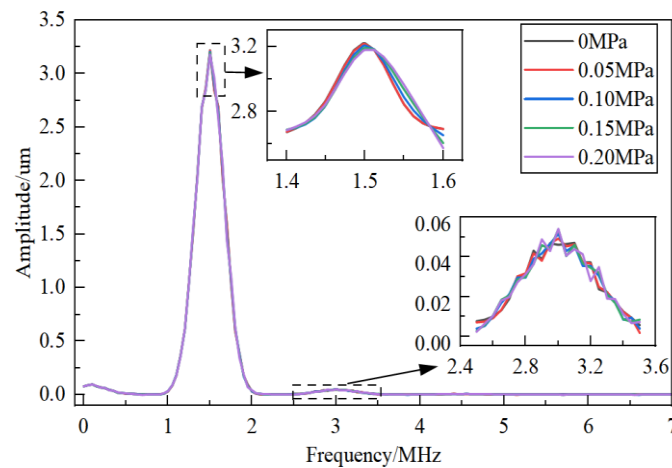


Figure 6. Silicon rubber-XLPE interface-reflected wave spectrum at different pressures.

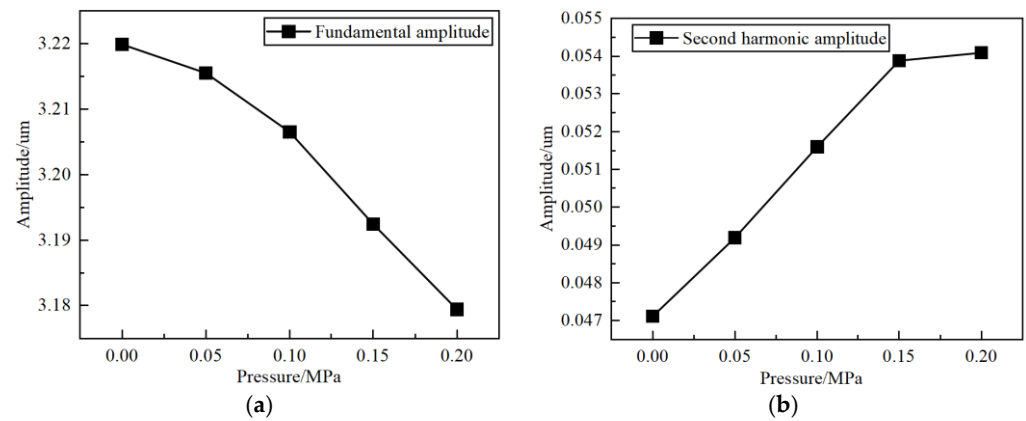


Figure 7. Curves of the fundamental and second harmonic amplitudes of reflected waves at the silicone rubber-XLPE interface as a function of pressure. (a) Fundamental wave amplitude variation curve. (b) Second harmonic amplitude variation curve.

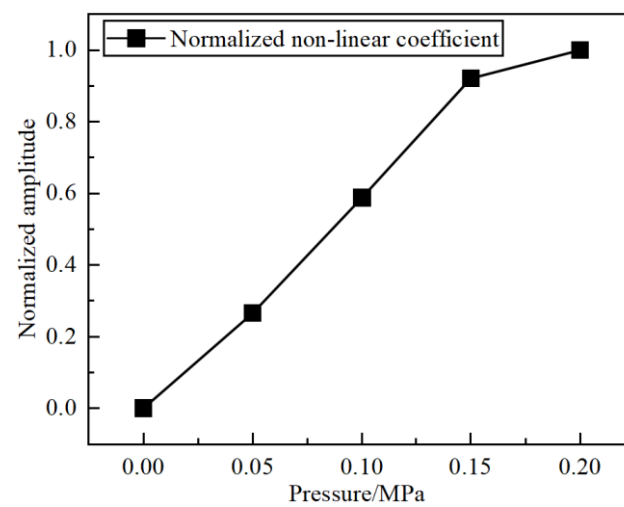


Figure 8. Relationship between ultrasonic nonlinearity coefficient and pressure at the silicone rubber-XLPE interface.

3. Materials and Methods

3.1. Specimens

Based on the actual structure of the YJJJ12 110 kV silicone rubber monolithic prefabricated cable intermediate joints, produced by Guodian Changyuan Electric Power Co., Ltd. (Wuhan, China), the cylindrical physical shape was simplified to a flat specimen. The test samples were prepared by the cable accessories manufacturer, Guodian Changyuan Electric Power Co., Ltd., using standard production equipment and raw materials, where the silicon rubber material and XLPE insulation material used in the samples were processed in the same way as 110 kV prefabricated cable intermediate joints. The size of the silicone rubber was 100 mm × 100 mm × 15 mm, and the size of the XLPE was 10 mm × 100 mm × 9 mm, as shown in Figure 9.



Figure 9. Experimental materials. (a) Silicon rubber and (b) XLPE.

3.2. Experimental Setup

The test system consists of a RAM-5000 SNAP nonlinear, high-energy ultrasonic test system, a 50 Ω impedance matcher, a duplexer, a low-pass filter bank, a band-pass filter bank, an oscilloscope, and a computer. In order to receive more harmonic components from the reflected waves at the interface, a longitudinal ultrasonic transducer from Olympus from Changsha Pengxiang Electronic Technology Co. (Changsha, China) with a central frequency of 2.25 MHz was selected for this test, and the bandwidth of the transducer met the test requirements. The pressure measurement device consists of a pressure transducer and a power supply. The pressure platform consists of a hydraulic press, bolts, nuts, springs, and an epoxy resin plate. The pressure value at the silicone rubber-XLPE interface is the product of the pressure sensor indication and the force area of the silicone rubber, as shown in Figure 10.

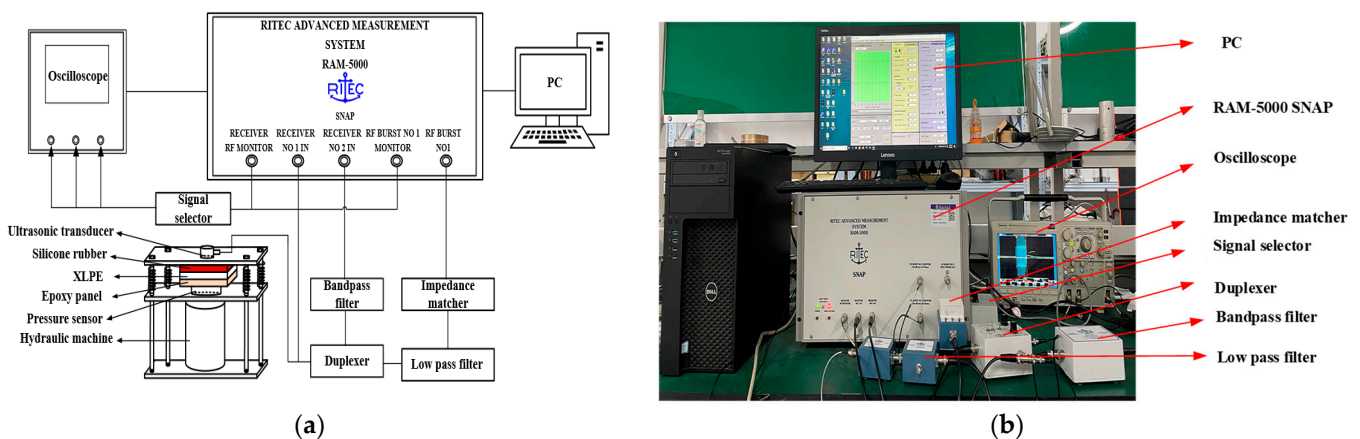


Figure 10. Nonlinear ultrasonic test stands. (a) Diagram of the test platform. (b) View of the test site.

The signal source excited by the system host is passed through a low-pass filter bank, in which the high-frequency signals are filtered out to ensure that the harmonic signals in the interface-reflected waves are not related to the input signal. The primary echo signal containing all frequency components is transmitted directly back to the system host reception port 1 through the duplexer, and the harmonic signal is transmitted back to the system host reception port 2 through the band-pass filter bank.

Silicone rubber is a high acoustic attenuation material, and for the same frequency of ultrasound, the longitudinal wave has less attenuation and better penetration than the transverse wave, so the longitudinal wave was chosen for the test. In order to receive more of the harmonic components of the reflected waves at the interface, an Olympus longitudinal ultrasound transducer with a central frequency of 2.25 MHz was chosen for this test.

The system was setup by computer software to generate a Hanning window-modulated signal of 2.25 MHz and 8 cycles. Glycerol was uniformly applied to the surface of the ultrasonic transducer and the sample under test to reduce the energy attenuation of the ultrasonic waves and the nonlinearity introduced by the coupling agent. The hydraulic device was controlled so that the pressure transducer indicated a gradient from 0 MPa to 0.2 MPa, in 0.05 MPa increments. Since it takes at least 30 min for the actual cable attachment to stabilize at the interface, a wait of 30 min was needed after each gradient before performing ultrasonic testing.

Since the coupling between the ultrasonic transducer and the pattern surface, the test equipment, and other factors will affect the test results, it is necessary to verify the reliability of the test system. Keeping the silicone rubber-XLPE interface pressure unchanged at a certain value, the excitation voltage of the system was gradually increased, and the relationship between the fundamental amplitude, A_1^2 , and the harmonic amplitude, A_2 , under different excitation voltages was obtained, as shown in Figure 11. The fitting curve formula was: $A_2 = 1.2584103A_1^2 + 0.0592$, and the correlation coefficient, R^2 , was 0.993. It can be seen that when the excitation voltage increased, A_2 and A_1^2 had a good linear relationship, and the stability of the test system was high.

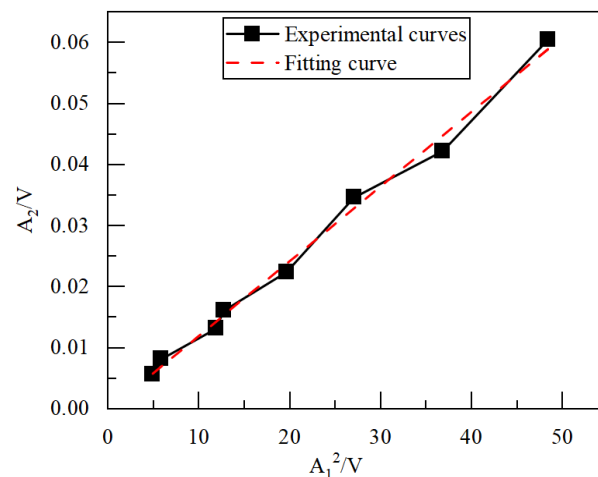


Figure 11. Relationship between the second harmonic amplitude A_2 and A_1^2 .

3.3. Experimental Results and Analysis

Nonlinear ultrasonic testing of the pressure at the silicone rubber-XLPE interface was carried out using the test setup and the test method described above. The waveform obtained from the test when no external pressure was applied is shown in Figure 12.

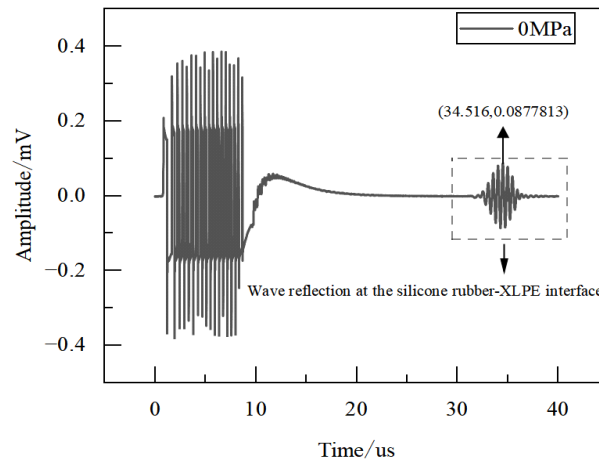


Figure 12. Reflected waveform at the silicone rubber–XLPE interface.

Based on the relationship between time, sound velocity, and propagation distance for the interface-reflected waveform verification in Figure 10, according to Equation (10) [25]:

$$2h = v(t_2 - t_1) \tag{10}$$

where:

- h is the thickness of the silicone rubber,
- v is the speed of sound propagated in the silicone rubber,
- t_1 is the front signal time, 0.732 μ s,
- t_2 is the reflected signal reception time, 31.448 μ s.

Through calculation, it can be concluded that the time domain waveform of 30–40 μ s in Figure 12 is the primary echo of the silicone rubber-XLPE interface. The spectrum was obtained by Fourier transforming the silicone rubber-XLPE interface echoes in Figure 12, as shown in Figure 13. The second harmonic signal appeared in the spectrogram after the ultrasonic waves were reflected by the silicone rubber-XLPE interface. This indicates that the interaction of ultrasound with the nonlinear features of the interface produced a nonlinear effect.

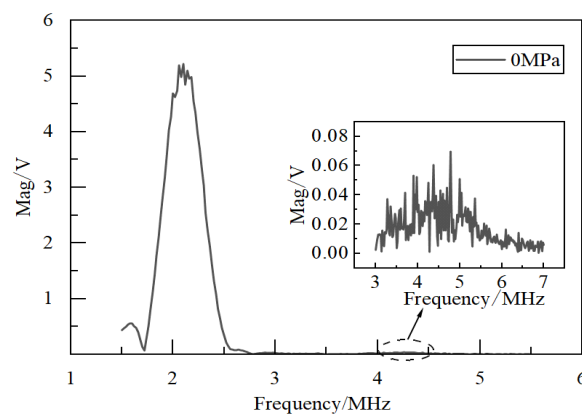


Figure 13. Reflected wave spectrum at the silicone rubber-XLPE interface.

Figure 14a shows the variation curve of the fundamental wave amplitude of the interfacial-reflected waves at different pressures. Figure 14b shows the variation of the second harmonic amplitude of the interface-reflected wave at different pressures. According to Equation (8), the ultrasonic nonlinear coefficient of the interface-reflected wave at different pressures was calculated, and its variation law with pressure is shown in Figure 15.

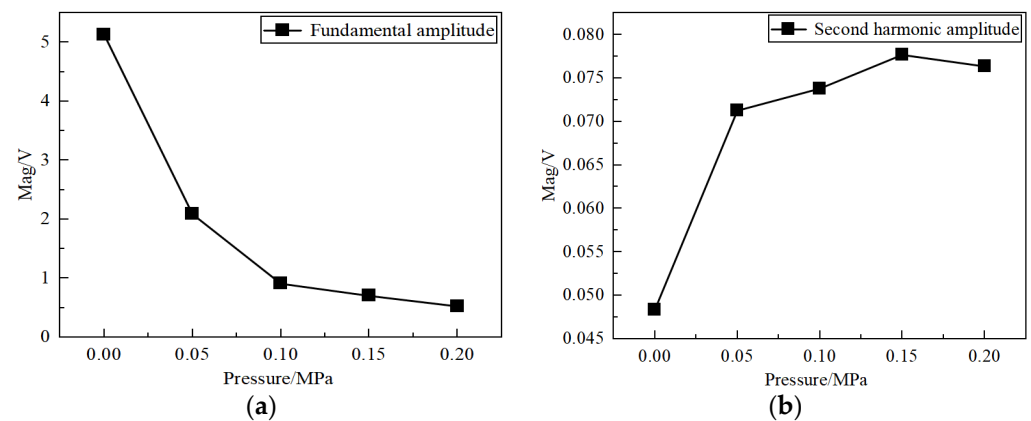


Figure 14. Curves of fundamental and second harmonic amplitudes of reflected waves at the silicone rubber-XLPE interface as a function of pressure. (a) Fundamental wave amplitude variation curve. (b) Second harmonic amplitude variation curve.

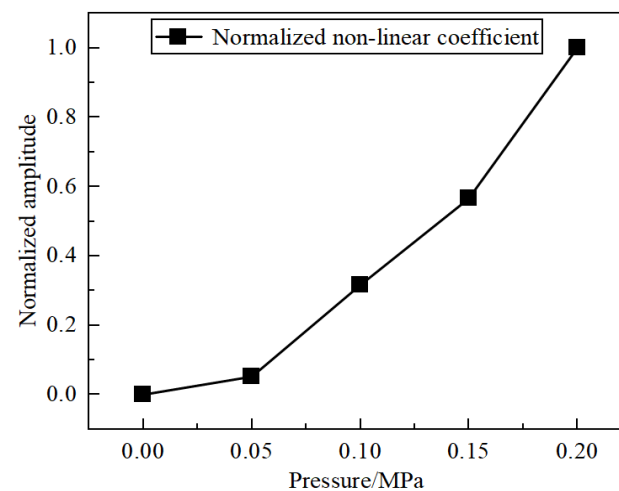


Figure 15. Silicone rubber-XLPE interface ultrasonic nonlinearity coefficient as a function of pressure.

As shown in Figure 14a, the fundamental wave amplitude decreased as the contact pressure at the interface increased. This is because the pressure increased the actual contact area of the interface, and the enhancement of the transmitted wave caused the reflected wave to weaken. As shown in Figures 14b and 15, the second harmonic amplitude increased, and the ultrasonic non-linear coefficient also increased as the interface pressure increased. The reason for this is that the compressive stress reduced the gap between the interfaces, enhancing the generation of second harmonics and the contact nonlinearity at the silicone rubber-XLPE interface.

As the contact interface studied in this paper consisted of two different materials, the ultrasonic transducer was placed on the XLPE surface and tested again in order to investigate whether the materials had an effect on the test results. The relationship between the ultrasonic non-linear coefficient and the pressure at the interface is shown in Figure 16. As the interface pressure increased, the relative nonlinearity coefficient tended to increase overall, and the relative nonlinearity coefficient increased more and more rapidly at equal pressure changes, due to the interface microstructure changing its contact state more under pressure.

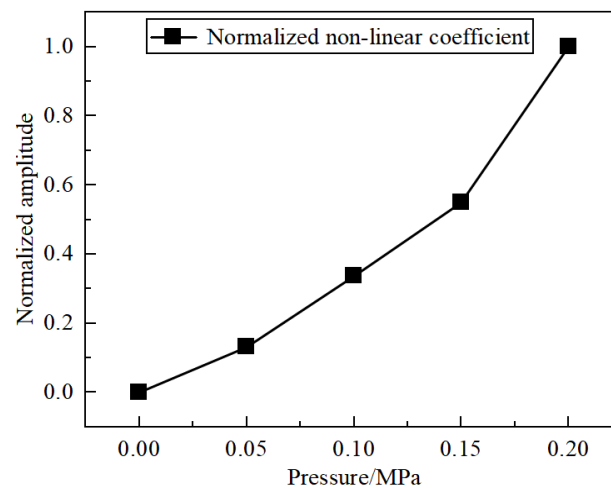


Figure 16. XLPE–silicone rubber interface ultrasonic nonlinearity coefficient as a function of pressure.

3.4. Comparison of Simulation and Experimental Results

The theoretical values of the interfacial nonlinear coefficient were compared with the experimental values, as shown in Figure 17. As the pressure at the silicone rubber-XLPE interface increased, the theoretical and experimental values followed the same general trend. It can be seen that the experimental value of the nonlinear coefficient was smaller than the simulated value, which may be attributed to the fact that the pressure at the interface of silicone rubber-XLPE was smaller than the pressure value displayed by the pressure transducer, resulting in a smaller change in the fundamental and second harmonic amplitudes. The nonlinear coefficient showed approximately the same trend as the pressure variation when ultrasound was incident from the silicone rubber surface and the XLPE surface, respectively. This indicates that for contact interfaces made up of different materials, the surface from which the ultrasound is incident has less influence on the results of the interfacial nonlinear coefficient.

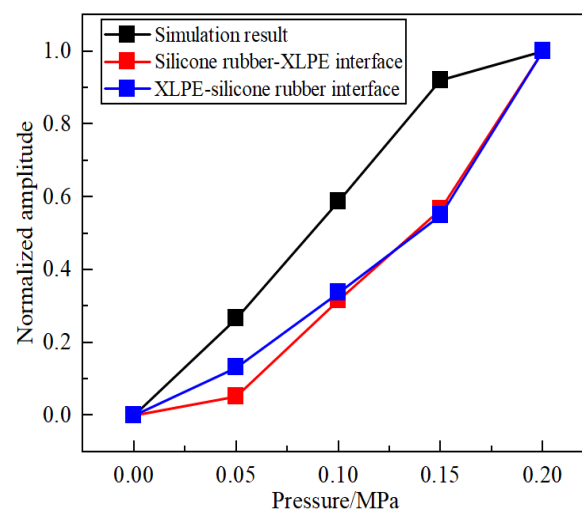


Figure 17. Comparison of theoretical and experimental interface nonlinearity coefficients.

4. Conclusions

In this paper, nonlinear ultrasonic detection of the pressure at the silicone rubber-XLPE interface was performed by simulations and experiments, and the results showed that:

- (1) As the interface pressure increased, the time domain amplitude of the reflected waves at the interface slightly decreased, the fundamental amplitude of the interface-reflected wave frequency domain decreased, the second harmonic amplitude increased, and the ultrasonic nonlinear coefficient increased.

- (2) For contact interfaces composed of two different materials, ultrasound waves were vertically incident to the interface from both sides, and the nonlinear ultrasound detection results were approximately the same.
- (3) The use of the relative nonlinear coefficient could effectively achieve evaluation of the pressure state of the flat silicone rubber interface, which provided a new idea for the pressure detection of the interface between the actual cable accessories and the cable body.

The authors' use of nonlinear ultrasound techniques allowed for the detection of flat silicone rubber-XLPE interfacial pressures, which provides a basis for research into the detection of interfacial pressure in real products. The shape of the real product resembles a cylindrical shape, and the ultrasonic transducer needs to use a curved probe when performing nonlinear ultrasonic inspection. Alternatively, a device that can be fully coupled to the curved surface of the real sample can be designed so that the curved coupling device is paired with a planar ultrasound transducer for detection. Based on the relationship between the nonlinear coefficient and the interfacial pressure, the magnitude of the interfacial pressure can be deduced from the nonlinear coefficient.

However, in the simulation, the authors used equally spaced and sized semicircles to characterize the roughness of the silicone rubber surface, which simplified the silicone rubber-XLPE interface contact state to some extent. The modeling of the silicone rubber-XLPE interface can be improved later to bring it closer to the real situation. During the actual operation of the cable intermediate joint, factors such as interface roughness, temperature, ageing, overfill, and the coupling agent all affect the interface pressure between the cable attachment and the body. The authors have only studied one sample of roughness value in this article so far, and the relationship between the interfacial pressure and the nonlinear coefficient needs to be continued to be investigated for different roughness values. There is also a need to continue to explore the effects of temperature, ageing, and other factors on the nonlinear ultrasonic detection of silicone rubber-XLPE interfacial pressure. In this paper, only a simplified model of 110 kV integral prefabricated cable accessories was investigated. Subsequent studies on cable intermediate joints for medium- and low-voltage distribution networks (e.g., wrapped, cold-shrink, heat-shrink cable intermediate joints, etc.) can be carried out.

Author Contributions: Conceptualization, C.F.; methodology, C.F., A.S. and J.L.; validation, A.S. and J.W.; formal analysis, A.S.; investigation, C.F., J.L., A.S. and J.W.; data curation, C.F., J.L., A.S. and Y.Z.; writing—original draft preparation, A.S., Y.Z. and F.L.; writing—review and editing, C.F., J.L. and J.W.; visualization, C.F., R.X. and F.L.; supervision, C.F., J.L., R.X. and B.O.; project administration, C.F. and J.L.; funding acquisition, J.L. and R.X. All authors have read and agreed to the published version of the manuscript.

Funding: This research was supported by the Open Fund of the State Key Laboratory of Power Grid Environmental Protection (GYW51202201415).

Data Availability Statement: All relevant data are included in the paper.

Acknowledgments: This research was supported by the State Key Laboratory of Power Grid Environmental Protection.

Conflicts of Interest: The authors declare no conflict of interest.

References

1. Liu, C.; Hui, B.J.; Fu, M.L.; Liu, T.; Hou, S.; Wang, X.Y. Influence of Mechanical Stress on the Operation Reliability of Silicone Rubber High Voltage Cable Accessories. *Gaodianya Jishu/High Volt. Eng.* **2018**, *44*, 518–526.
2. Fournier, D.; Dang, C.; Paquin, L. Interfacial Breakdown in Cable Joints. In Proceedings of the 1994 IEEE International Symposium on Electrical Insulation, Pittsburgh, PA, USA, 5–8 June 1994.
3. Wang, X.; Dong, Y.; Duan, S.; Zhang, Y.; Zhang, W.; Wu, K.; Tu, D. Dealing with Some Key Design Problems in Hv Cable Accessory. *Gaodianya Jishu/High Volt. Eng.* **2018**, *44*, 2710–2716.

4. Dang, C. Effects of Aging on Dielectric Interfaces of Cable Accessories. In Proceedings of the Conference Record of the 1998 IEEE International Symposium on Electrical Insulation (Cat. No.98CH36239), Arlington, VA, USA, 7–10 June 1998.
5. Jia, Z.; Zhang, Y.; Fan, W.; Zhu, B.; You, J.; Lu, G. Analysis of the Interface Pressure of Cold Shrinkable Joint of 10 Kv Xlpe Cable. *Gaodianya Jishu* **2017**, *43*, 661–665.
6. Wang, X.; Wu, C.; Wang, Y.; Fan, Z.; Wu, K. Double Optical Fiber Temperature Compensation Method for Measurement of Interface Pressure between Simulated Cable and Accessory at High Temperatures. *IEEE Trans. Dielectr. Electr. Insul.* **2023**, *1*. [[CrossRef](#)]
7. Wang, X.; Fan, Z.; Wu, C.; Wu, K. External Fiber Grating Sensor Used for Measurement of Interface Pressure between Cable and Accessory. *Gaodianya Jishu/High Volt. Eng.* **2022**, *48*, 38–46.
8. Tian, Z.; Sun, L.; Wang, J.; Bai, X. A Study of Simulation on Relationship between Young's Modulus of Cable Joints and Interface Pressure Based on Finite Element Method. Presented at the 2018 International Symposium on Power Electronics and Control Engineering, ISPECE 2018, Xi'an, China, 28–30 December 2018.
9. Zhang, D.; Han, Y.; Liu, H.; Shen, W. Determination of the Pressure Distribution at the Xlpe Cable-Rubber Interface in a Self-Pressurized Joint. *Gaodianya Jishu/High Volt. Eng.* **2007**, *33*, 173–176.
10. Ma, Y.-Q.; Zheng, P.; Han, X.; Xu, C. Measurement and Analysis of Insulated Interfacial Pressure of Cable Termination in Installation & Operation. *Gaodianya Jishu/High Volt. Eng.* **2011**, *37*, 347–353.
11. Chen, J.; Jiang, W.; Shui, Y. Experimental Studies of Nonlinear Reflection on Isotropic Solid Interface. *Shengxue Xuebao* **1999**, *24*, 137–142.
12. Liu, M.; Qu, J.; Kim, J.-Y.; Jacobs, L. Measuring Surface Stress Using Nonlinear Ultrasound. In Proceedings of the SAMPE 2010 Conference and Exhibition New Materials and Processes for a New Economy, Seattle, WA, USA, 17–20 May 2010.
13. Wang, M.; Pau, A. Stress Monitoring Ofplates Bymeans Ofnonlinear Guided Waves. Presented at the 10th European Workshop on Structural Health Monitoring, EWSHM 2022, Palermo, Italy, 4–7 July 2022.
14. Jiang, H.; Zhang, J.; Jiang, R. Stress Evaluation for Rocks and Structural Concrete Members through Ultrasonic Wave Analysis: Review. *J. Mate. Civ. Eng.* **2017**, *29*, 04017172. [[CrossRef](#)]
15. Yan, H.J.; Xu, C.G.; Xiao, D.G.; Cai, H.C. Research on Nonlinear Ultrasonic Properties of Tension Stress in Metal Materials. *Jixie Gongcheng Xuebao* **2016**, *52*, 22–29. [[CrossRef](#)]
16. Jiao, J.; Li, L.; Gao, X.; Cheng, Q.; He, C.; Wu, B. Application of Nonlinear Lamb Wave Mixing Method for Residual Stress Measurement in Metal Plate. *Chin. J. Mech. Eng. Engl. Ed.* **2023**, *36*, 12. [[CrossRef](#)]
17. Kim, Y.; Choi, S.; Jhang, K.Y.; Kim, T. Experimental Verification of Contact Acoustic Nonlinearity at Rough Contact Interfaces. *Materials* **2021**, *14*, 2988. [[CrossRef](#)] [[PubMed](#)]
18. Mao, H.; Zhang, Y.; Mao, H.; Li, X.; Huang, Z. Stress Evaluation of Metallic Material under Steady State Based on Nonlinear Critically Refracted Longitudinal Wave. *Results Phys.* **2018**, *9*, 665–672. [[CrossRef](#)]
19. Yan, H.J.; Liu, F.B.; Pan, Q.X. *Nonlinear Ultrasonic Properties of Stress in 2024 Aluminum*; Trans Tech Publications: Guilin, China, 2017.
20. Payan, C.; Garnier, V.; Moysan, J.; Johnson, P.A. Determination of Nonlinear Elastic Constants and Stress Monitoring in Concrete by Coda Waves Analysis. *Eur. J. Environ. Civ. Eng.* **2011**, *15*, 519–531. [[CrossRef](#)]
21. Jiao, J.; Zeng, X.; Zhang, Q.; He, C.; Wu, B. Micromechanical Model of Rough Surface for Evaluation of Acoustic Properties of Pressure Interfaces. *Jixie Gongcheng Xuebao* **2011**, *47*, 78–83. [[CrossRef](#)]
22. Jiao, J.-P.; Zeng, X.-C.; Liu, W.-H.; He, C.-F.; Wu, B. Ultrasonic Testing on Contact State of Pressure Interfaces. *Beijing Gongye Daxue Xuebao* **2012**, *38*, 807–812.
23. Biwa, S.; Nakajima, S.; Ohno, N. On the Acoustic Nonlinearity of Solid-Solid Contact with Pressure-Dependent Interface Stiffness. *J. Appl. Mech. Trans. ASME* **2004**, *71*, 508–515. [[CrossRef](#)]
24. Wang, S.; Yao, X.F.; Yang, H.; Huang, S.H. Measurement and Evaluation on Contact Stress at the Rubber Contact Interface. *Measurement* **2019**, *146*, 856–867. [[CrossRef](#)]
25. Jeong, J.J.; Choi, H. An Impedance Measurement System for Piezoelectric Array Element Transducers. *Measurement* **2017**, *97*, 138–144. [[CrossRef](#)]

Disclaimer/Publisher's Note: The statements, opinions and data contained in all publications are solely those of the individual author(s) and contributor(s) and not of MDPI and/or the editor(s). MDPI and/or the editor(s) disclaim responsibility for any injury to people or property resulting from any ideas, methods, instructions or products referred to in the content.